

Supporting Information

Mass Activated Droplet Sorting (MADS) Enables High-Throughput Screening of Enzymatic Reactions at Nanoliter Scale

Daniel A. Holland-Moritz, Michael K. Wismer, Benjamin F. Mann, Iman Farasat, Paul Devine, Erik D. Guetschow, Ian Mangion, Christopher J. Welch, Jeffrey C. Moore, Shuwen Sun,* and Robert T. Kennedy**

ange_201913203_sm_miscellaneous_information.pdf

ange_201913203_sm_S1_Reinjection.avi

ange_201913203_sm_S2_ReagentAddition.avi

Author Contributions

D.H. Formal analysis: Lead; Investigation: Lead; Methodology: Lead; Software: Supporting; Validation: Lead; Writing—Original Draft: Lead; Writing—Review & Editing: Lead

M.W. Methodology: Supporting; Software: Lead; Writing—Original Draft: Supporting

B.M. Methodology: Supporting; Writing—Review & Editing: Supporting

I.F. Investigation: Supporting

E.G. Methodology: Supporting

S.S. Conceptualization: Lead; Funding acquisition: Lead; Investigation: Lead; Methodology: Lead; Project administration: Lead; Supervision: Lead; Writing—Review & Editing: Lead

J.M. Conceptualization: Lead; Funding acquisition: Lead; Methodology: Lead; Project administration: Lead; Writing—Review & Editing: Lead

R.K. Conceptualization: Lead; Funding acquisition: Lead; Project administration: Lead; Supervision: Lead; Writing—Review & Editing: Lead

I.M. Supervision: Supporting

C.W. Supervision: Supporting

P.D. Supervision: Supporting.

Table of Contents**Experimental Procedures**

Device Fabrication	3
Fluid Flow Control	3
Droplet Storage and Reinjection	3
Droplet Imaging	4
MS Conditions for Droplet Analysis	4
Reagent Addition Device Operation	4
MADS Device Operation	4
DEP Sorting and Imaging Analysis	5
ivTT Reaction Conditions	5
Error Tolerance	7
Electronics	8
Chemicals	9
Transaminase Plasmid Sequence: pUC57 – Kan	10

Supplemental Data

Enzyme Assay and Activity	11
Droplet Leakage	12
Extended Operation	13
Sorting Ratio	14
Description of Supplemental Videos	15

Author Contributions

16

Experimental Procedures

Device Fabrication

Microfluidic devices were fabricated using standard soft lithography techniques^[1]. Devices were designed using AutoCAD software (Autodesk) and printed onto mylar film masks at 25000-50000 dpi (Fineline Imaging). Using these masks, SU-8 2075 (Microchem Corp) was patterned to a depth of 200 μm on a 7.62 cm (3 in) diameter silicon wafer (University Wafer). PDMS (RTV 615, Curbell Plastics) was prepared in a 1:10 ratio of activator to monomer, poured over the wafers and cured 1 h at 70 °C before it was removed from the mold and hard baked for 1 hour at 120°C. Punched ports were created in the cured PDMS using a sharpened 20 or 22 ga syringe needle (BD) and the punched holes were cleaned by passing a short length of fused silica capillary (360 μm OD, 20 μm ID, Molex) through the hole to clear any particulate left behind by the punch.

Devices were cleaned with Scotch tape (3M) and bonded to 7.62 cm long (3 x 1 in) glass microscope slides (Corning) after exposing both the slide and the molded PDMS to oxygen plasma for 15 s each using a corona discharge wand (Electrotechnics). Bonded devices were placed in an oven to cure at 80 °C. Within 10 min of bonding, chips were flushed with a derivatization solution of trichloro(1H,1H,2H,2H-perfluorooctyl)silane (Sigma-Aldrich) dissolved 2% by volume in perfluorodecalin (95%, Sigma-Aldrich). Flushed devices were baked overnight at 70 °C.

Fluid Flow Control

When using syringe pumps to drive fluid flow, Hamilton Gastight glass syringes were connected to Teflon (PFA) tubing using 250 μm ID PEEK unions (Valco). 30 ga Teflon tubing was sheathed in 1/16" OD, 1/32" ID Teflon tubing (Cole Parmer) to allow the 1/16" Peek union ferrule to grip the smaller diameter tubing. These syringes were driven using a Harvard Apparatus PHD syringe pump. When using gas pressure to drive fluid flows onto a device, sealed autosampler vials (Chemglass Lifesciences) were pressurized using an Elveflow OB1-Mk3 pressure pump. Tygon tubing running from the pressure pump was connected to syringe needles via luer-lock connectors and these were inserted into the vial septa. 30 ga thin wall Teflon tubing (Cole Parmer) inserted through the same vial septa allowed fluids to exit the vials and flow onto the microfluidic devices when the vial headspace was pressurized.

Droplet Storage and Reinjection

Droplets were collected in a custom built storage chamber made from an 8 cm Pasteur pipette with the tapered tip removed (Figure S1). Silicone or rubber stoppers (00, Fisher) were cut with biopsy punches (6 mm, Fisher) to cap the ends and access holes were cut to allow the insertion of 30 ga Teflon tubing through the caps. During chamber filling, tubing from the droplet generation or reagent addition device was inserted into the bottom of the chamber, allowing generated droplets to flow directly into the chamber. A second segment of tubing inserted into the bottom of the chamber allowed excess oil to be drained off. During chamber emptying, this second segment was tied off and the first was used to pump oil into the chamber. With no available escape through the bottom of the chamber, droplets flow out through the tubing at the top of the chamber.

During extended incubation (>3 h), oil was circulated through the container by drawing oil from the bottom of the chamber and simultaneously pumping replacement oil in through the upper tubing. Oil was circulated using a Masterflex L/S peristaltic pump (Cole Parmer).

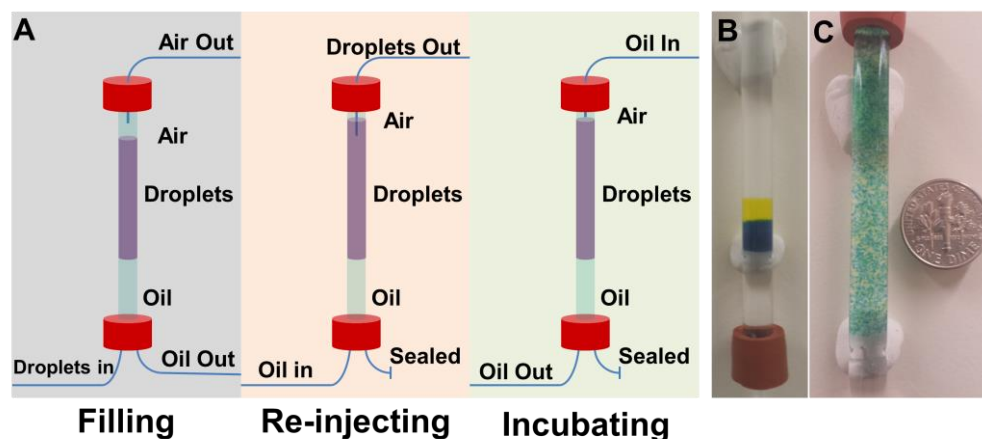


Figure S1. (A) Operating modes for the custom droplet storage chamber. (B) Droplets may be stored in layers as generated or (C) mixed by circulating oil in incubation mode.

Droplet Imaging

During device operation, droplet size, frequency, color, and contents were monitored using one of two cameras. For high speed monitoring of droplet formation or similar high frequency events, a Phantom Miro C110 high speed camera was connected to a Nikon TS2-FL microscope. During MS-directed droplet sorting, a Cognex 7600C image sensor connected to the same microscope was used to monitor the droplets exiting the device to track and count droplets prior to sorting.

MS Conditions for Droplet Analysis:

Droplet analysis was performed using an Agilent single quadrupole mass spectrometer (6120b). Droplets were directly infused from the sorting device into the mass spectrometer through a 360 μm OD Teflon capillary directly inserted into a commercial Agilent CE-MS source^[2]. Parallel sheath flow composed of deionized water was driven by a Harvard Apparatus PHD syringe pump and a 10 mL Hamilton gastight syringe at 30 $\mu\text{L}/\text{min}$. Capillary voltage was 3 kV, with 350 °C drying gas set at 30 L/min and a source pressure of 10 psi. Single ion monitoring was used to track the small molecules (Table S1) pyridinyl amine (m/z 123.0), ATA substrate amine (m/z 182.0), carnitine (m/z 162.3), neostigmine (m/z 223.0), and chlorocholine (m/z 122.3). Peak height (MS dwell time) was set to 0.005s.

Reagent Addition Device Operation:

Reagent addition is driven using a combination of gas pressure and syringe pumps to drive fluid flow. To ensure 1 nL droplets flow on to the device at a steady rate, a 500 μL Hamilton gastight syringe is used to flow perfluorinated oil at 0.5-1.0 $\mu\text{L}/\text{min}$ into the bottom of the droplet storage chamber, driving droplets out through tubing inserted into the top (Figure S1). Meanwhile, the gas pressure pump is used to pressurize two vials to 2 psi (13.8 kPa). One vial is used to hold the perfluorinated carrier phase for droplet generation while the other holds the aqueous sample used for droplet generation. The pressure on the vial of aqueous material is adjusted to create droplets of a pre-determined size at the flow focusing region of the device, while the syringe pump flow rate is adjusted to match the frequency of 1 nL droplet introduction to the frequency of droplet generation. Paired droplets flow downstream past two salt water^[3] channels where an applied 1.5 kV AC field merges the two droplets (Video S2). Exiting droplets flow directly into a second droplet storage chamber. This allows droplets to be transferred from device to device without ever necessitating the use of a pipette which may shear large 30 nL samples.

MADS Device Operation:

Flow in the MADS chip is driven by a combination of syringe pumps and gas pressure. A 10 mL Hamilton syringe filled with perfluorinated oil respaces droplets as they enter the device (Video S1) while a 1 mL syringe drives oil into the storage chamber and droplets onto the device. Both syringes are driven by a single syringe pump, programmed to push the 1mL syringe at 1.5 $\mu\text{L}/\text{min}$. Thus, the net flow onto the device is 16.5 $\mu\text{L}/\text{min}$, Droplets entering the device are spaced with oil at a 1:10 ratio.

Due to the differences in back pressure between the MS and sorting exits of the device, the sorting outlet vials and the sorting region are held at elevated pressure. To do this, a pressurized vial drives oil into an inlet in the device located at the end of the delay line but prior to the sorting junction (Figure S2). The sorting bifurcation flows into two vials that are pressurized equally using a T-split line from the gas pressure pump. The difference in pressure between the oil vial and the collection vials dictates the velocity of droplet flow through the sorting region, and may be used to accelerate droplets as they enter the sorting region. Typically, this pressure drop is held at 0.2 psi (1.4 kPa).

The applied pressures at the sorting region of the device must be slowly ramped as the device begins to operate and the two exit paths are filled with droplets. This ensures that both the on-chip delay line and the connected capillary maintain approximately equal back pressures as they fill with samples. Once both exits are filled and flowing at the same rate, the applied back pressure can be maintained indefinitely and the device will operate with minimal user input for as much as 6 h. We find the optimal operating back pressures for our system with a ~60 cm transfer capillary to be 1.2-1.6 psi (8.3-11 kPa) at the oil inlet, but this will vary depending on the input flow rates, exact capillary lengths, droplet composition, and the MS source pressure.

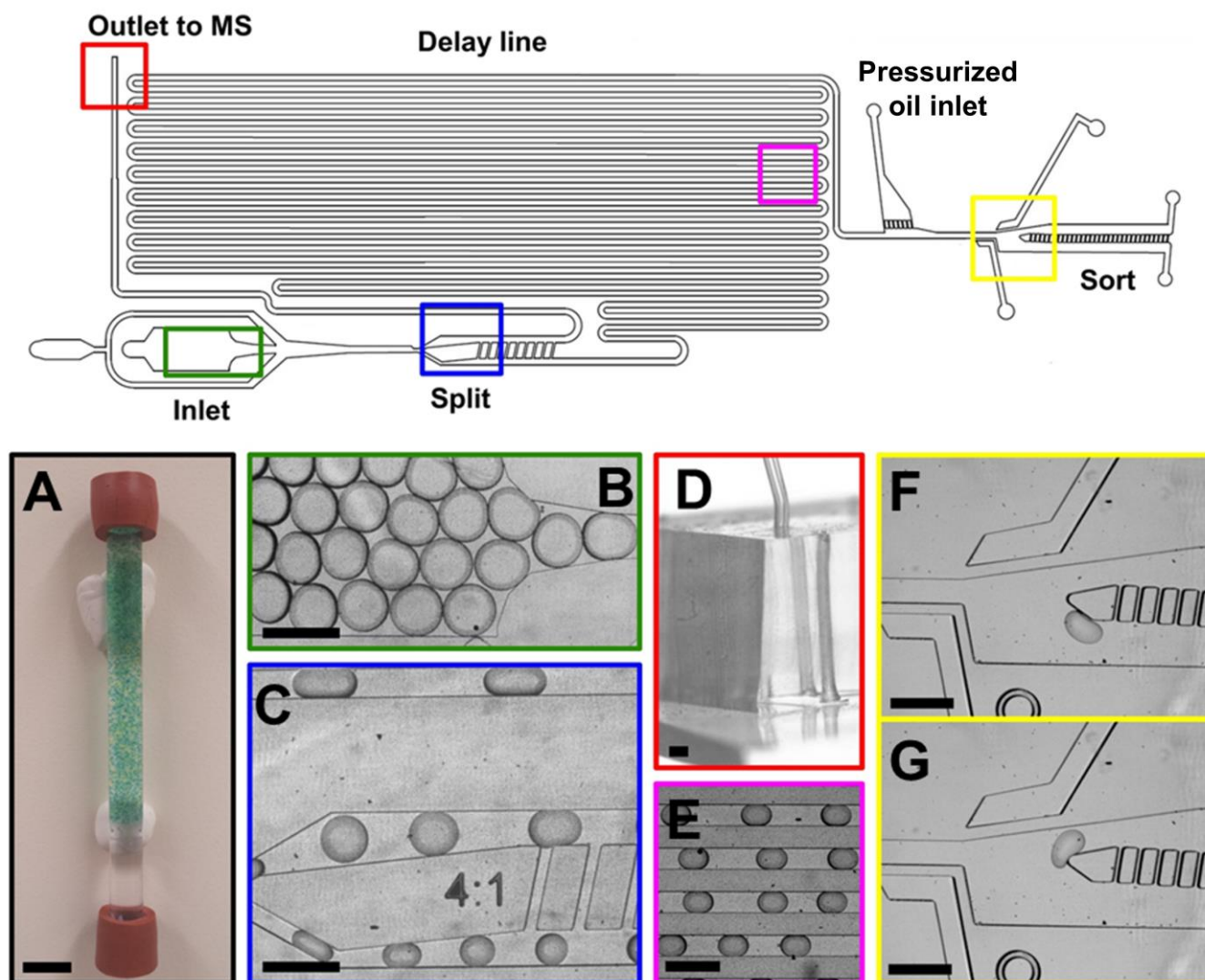


Figure S2. Schematic of the droplet sorting device. (A) ~25 nL droplets are stored in bulk prior to being pumped onto the device. (B) As they enter the microfluidic device, (C) droplets are split into two daughter droplets (Video S1). (D) The larger of the two halves leaves the device via an inserted Teflon capillary while (E) the smaller of the two remains on chip and is pumped into an extended delay line. After the larger droplet is sprayed, a 1.5 kV AC pulse at the sorting junction (F, G) directs droplets into one of two outlets. Scale bar in (A) is 1 cm, all others are 500 μm .

DEP Sorting and Imaging Analysis:

In simple sorting experiments of analyte in water, peak threshold voltages for sorting were set based off of the experimentally observed peak intensities from the first few droplets. In enzyme reaction sorting experiments, thresholding was set at 1.2-1.45 times the average signal from positive control droplets sprayed by the system.

If a sprayed droplet was determined to meet the sorting criteria, a high voltage AC pulse applied to the upper salt water electrode in the sorting region would pull it into the positive outlet; otherwise the droplet would be hydrodynamically directed to waste (Figure S2F). Collected pools of droplets were imaged on a Nikon TS2-FL with a Phantom Miro C110, and analyzed using imageJ software to determine sorting accuracy and enrichment. Positive “Hit” droplets could be confirmed via fluorescent imaging of the FAD-containing droplets which set them apart from the non-fluorescent marker and blank droplets. Excitation wavelength for FAD imaging was 470 nm (blue LED) and a 525 nm Nikon FITC filter cube was used to filter the emission.

ivTT Reaction Conditions:

Enzyme reactions were run by expressing transaminase DNA using New England Biolab’s PureExpress in vitro Transcription and Translation cell free expression system (ivTT). To make each dilution of ATA substrate amine in ivTT for the calibration experiments, 250 μL of cell free expression buffer was created from 100 μL and 75 μL respectively of solutions A and B (a proprietary mix of purified components of *E. Coli* protein translation), 10 μL of the RNase inhibitor murine (40000 units/mL, NEB), 10 μL of 2.5

mM Pyridoxal phosphate (PLP) in 10 mM TRIS (pH 7.5), and 1-(imidazo[2,1-b]thiazol-6-yl) propan-2-amine in nuclease free water such that seven final samples were created at 5 mM, 1 mM, 500 μ M, 250 μ M, 100 μ M, 50 μ M, and 0 μ M. Every other solution received 1 μ L of McCormick blue food dye to aid with visualization.

To make the stock solutions of ivTT to which DNA was added in our enzyme assays, 1 mL of cell free expression buffer was created from 400 μ L and 300 μ L respectively of solutions A and B, 40 μ L of RNase inhibitor, 40 μ L of 2.5 mM PLP in 10 mM TRIS, 20 μ L of nuclease free water, and 200 μ L 5 mM of 1-(imidazo[2,1-b]thiazol-6-yl) propan-2-amine and 5 mM pyruvic acid in 10 mM TRIS (pH 7.5). Final samples contained 1 mM ATA substrate amine, 100 μ M PLP cofactor, and 1 mM pyruvate. An identical 250 μ L solution of expression buffer was created for the marker droplets with the addition of 2.5 μ L blue McCormick food dye and 2.5 μ L of 50 mM L-carnitine in water to the 50 μ L 5 mM ATA substrate and pyruvic acid added.

1 nL droplets containing DNA (50 ng/ μ L final), FAD (5 mM final) and neostigmine (25 mM final) in water were formed using a commercial flow-focusing device (BioRad DG8). Upon addition to droplets of ivTT, these droplets express transaminase and are both visibly yellow and fluorescent. These small DNA droplets were pooled and mixed with blank water droplets and droplets containing 50 ng/ μ L WT plasmid and 50 mM chlorocholine. ivTT droplets that received these secondary DNA-containing droplets show activity, but not fluorescence and were used as a positive control signal for thresholding.

The combined pool of mixed 1 nL droplets contained all three varieties of droplet at a 1:1:6 ratio with the blanks making up the bulk. This mixed emulsion was reinjected into a device that segmented ivTT solution into ~25 nL volumes before pairing these larger volumes with a small droplet and merging them in a 1.5 kV AC electric field (Video S2).

Error Tolerance

MADS operation is dependent on the accurate alignment of two signals – that of the mass spectrometer, and that of the camera. Improper alignment produces false positives and non-alignment results in false negatives. Two parameters are critical to minimizing these events. The “minimum sync interval” determines the minimum number of samples between reset signals that the algorithm will attempt to align to. In this work, this was set to 5. If the interval is set too high, it takes much longer for an interval of the required length to occur, and more time will be spent un-synced. Too low, and the frequency of the shorter intervals will cause the system to align more frequently to the wrong interval, and sort incorrectly.

The second parameter is the “error threshold,” which in this work was set to 3. This value determines the stringency with which the MADS algorithm requires the intervals it logs in the synced state to align to the expected interval length. Frameshifts are possible when we allow this error threshold to be greater than 0, but the advantage is that the system is less likely to be thrown off by a single anomalous read by the camera or MS. Because the droplet sorting uses the marker droplets to reset the droplet count, any frame shift in the read will last only as long as the marker to marker interval during which the mistake is made. By allowing some leeway in the marker to marker count, we accept the possibility of brief frameshifts within a short marker to marker interval, but this shift is corrected the moment the next marker is read, and less time is spent trying to re-establish droplet alignment.

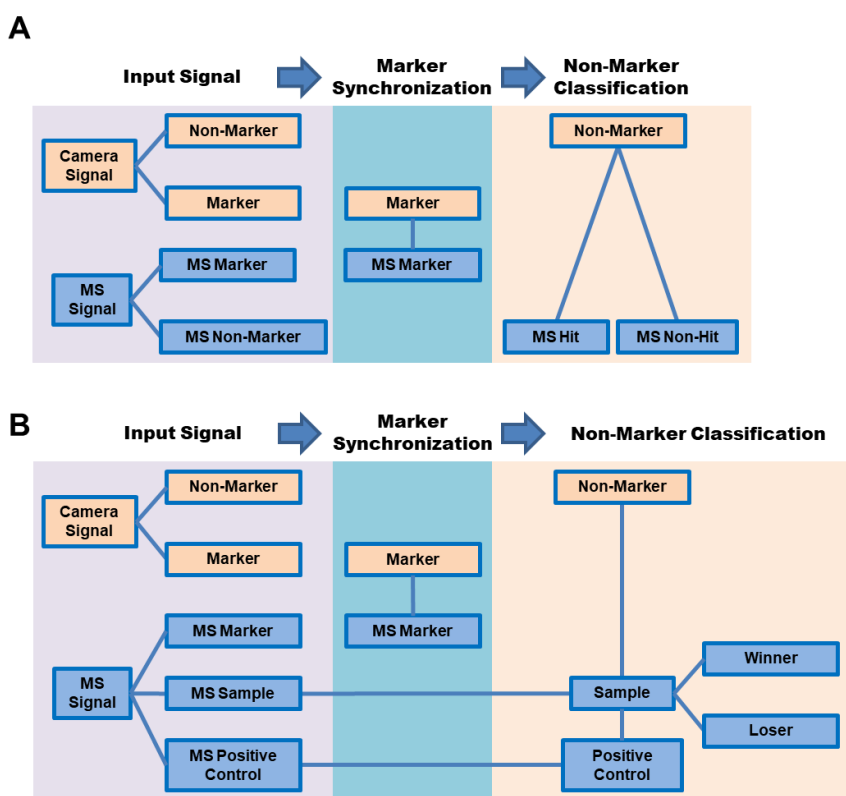


Figure S3. The MADS operating system was run in two decision making modes. In both modes, the alignment of the camera and the mass spectrometer is performed using marker droplets, allowing the synchronization of the non-marker droplets and enabling accurate sample tracking. (A) In the first mode of operation, droplet thresholding is based on a user defined threshold set at the beginning of operation, and “active” droplets are identified from among the non-marker droplets based on signal intensity above this threshold. (B) In the adaptive thresholding mode of operation, the addition of positive control samples into the droplet pool allows for dynamic adjustment of the “active” droplet threshold value as a function of the positive control signal. These positive control droplets are not targeted for sorting, and are tracked only by the mass spectrometer. The regular comparison of these control samples to the mock library samples allows the system to correct for any variation in signal over extended periods of operation.

Electronics:

Droplet signals from the electrospray of infused droplets are acquired from a four channel DAC card (Agilent G1960-67039) installed in the mass spectrometer. The frequency response of the DAC card was improved by removing the two $1\ \mu\text{F}$ capacitors from the lowpass filter stage for each 10x channel (figure S4). The 10x channels are used to provide better signal to noise performance. A standalone four channel programmable gain Bessel lowpass filter (Alligator USBPGF-S1/LX) is used to adjust signal gain and frequency response prior to acquisition. A Sigilent SDS 1104x-E oscilloscope was used to monitor and record signal outputs in real time. On the microscope, a machine vision camera with open collector logic outputs is used to visually identify droplets (Cognex 7600C).

A STM32F407 ARM Cortex M4 microcontroller board (Mikroelektronika 1685) runs custom software to synchronize the outputs from the mass spectrometer and the machine vision camera. The mass spectrometer outputs are wired into four 12-bit ADC inputs, and the open collector camera outputs are wired into two digital inputs with internal pull-ups. A digital output is used to control the DEP sorting voltage. This signal is buffered by a driver integrated circuit (Infineon IR2125), which selectively applies 5V power to a 1.5 kV AC 30 kHz cold cathode fluorescent lamp (CCFL) inverter board (JKL BXA-601). The outputs of the CCFL inverter are wired in parallel and connected through two 100k resistors in series to the sorting junction electrodes.

The microcontroller runs software written in C using Eclipse and ChiBiOS RTOS libraries. The microcontroller board is interfaced via USB to control software written in Labview on the host PC.

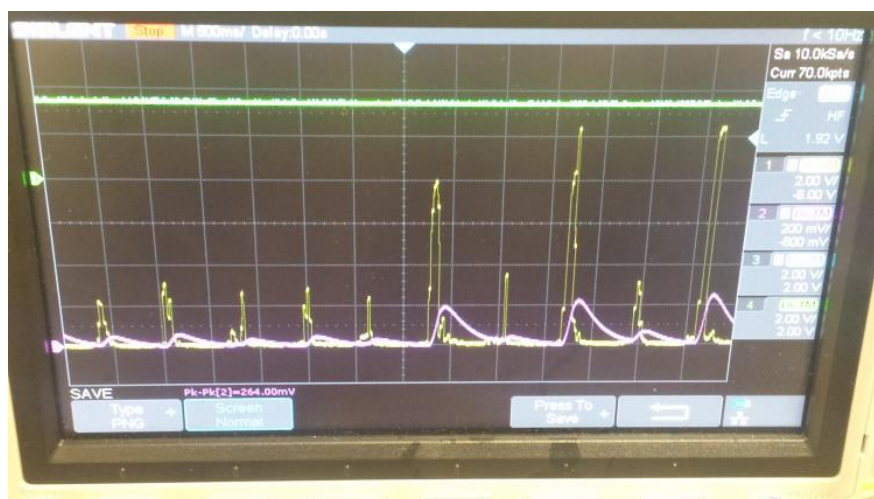
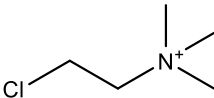
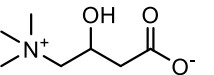
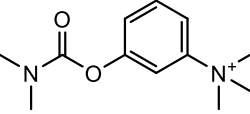
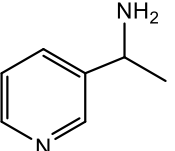
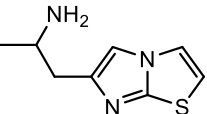
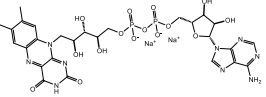
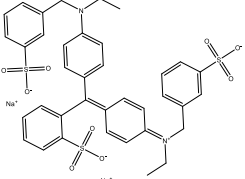


Figure S4: Agilent DAC board output viewed on the oscilloscope after modification. The yellow trace is the modified 10x output channel, and the magenta trace is the unmodified 1x output for the same channel. The yellow channel is shown at 2V/division, and the magenta channel is shown at 200mV/division, so that the displayed amplitudes are equivalent.

Chemicals:

All chemicals were purchased from Sigma Aldrich unless noted otherwise. Novec 7500 perfluorinated oil was purchased from 3M and Oakwood Chemical, surfactant 008 was purchased from RAN Biotechnologies, and ATA Substrate was purchased from Combi-Blocks, inc. Chemicals used for MADS alignment and to mark droplets are given in Table S1.

Table S1. Structures and uses for all small molecules monitored by mass spectrometry or imaging

Informal Name	Structure	MS signal ion or color	Use
Chlorocholine		m/z=122.3	Chemical Marker for WT control droplets
Carnitine		m/z = 162.3	Chemical signal for MADS Alignment
Neostigmine		m/z = 223.0	Chemical signal for model library droplets
"Pyridinyl amine"		m/z = 123.0	Chemical signal for hit droplets in basic sorting experiments
ATA Substrate		m/z = 182.0	Substrate monitored in transaminase reaction
Flavin Adenine Dinucleotide		Yellow and fluorescent	Visibly and fluorescently color target droplets for sorting
Blue Dye		Blue	Color signal for MADS alignment

Transaminase Plasmid Sequence: pUC57 - Kan

tcgcgcttccggtgatgacgggtgaaaacctctgacacatgcagctcccggagacgggtcacagctgtctgtaagcggatgccgggagcagac
aagcccgtcagggcgctcagcgggtgttggcgggtgtcgggctggcttaactatcgggcatcagagcagattgtactgagagtgcacatat
gcggtgtgaaataccgcacagatgcgtaaggagaaaataccgcatcagggcaccattcgccattcaggctgcgcaactgttgggaagggcgat
cggtcggggcctcttcgctattacgccagctggcgaaagggggatgtgctgcaaggcgattaagttgggtaacgccagggtttccagtcacg
acgttgtaaaacgacggccagtgaattgacgctattggatcaaggaatgggtcatgcaaggagctccgtagatagtcaaccaggcacagc
gaaattaatacactcactatagggagaccacaaccgccatatacggcgggacacacacaaggagaccatATGAAACAGAACAA
AGAACAGATCACCAAACAGAACATCAACGCGAGCTCTGCATTACAGCGCAGATACTAGCGAGATTG
TTTACACGCACGATACGGGTCTGGACTACATTACCTATAGCGACTATGAACTGGACCCGGCGAAT
CCGCTGGCTGGCGGCGCGGCCTGGATCGAGGGTGCATTCTCCGCCGTCCGAGGCGCGTATT
TCTATCTTTGACCAGGGTTATCTGCACAGCGACGTGACCTATACCGTGTCCACGTCTGGAACGG
TAATGCCTTTCTGTCTGGATGATCATATTGAGCGTCTGTTCTCTAACGCAGAGAGCATGCGCATTAT
CCCTCCGCTGACCCAAGATGAAGTGAAAGAAATTGCGCTGGAAGTGGTGGCCAAGACCGAGTTG
CGTGAGGCTTTCTGTTAGCGTTAGCATCACCCGCGGTTACAGCAGCACGCCGGGTGAGCGTGACA
TCACGAAGCACCGTCCACAAGTATACATGTACGCAGTGCCGTATCAGTGGATCGTGCCATTTGAT
CGCATTCTGTGATGGTGTCCACGCGATGGTTGCACAGTCCGTGCGCCGCACCCCTCGCAGCAGCA
TTGACCCGCAAGTCAAAAACCTCCAGTGGGGTGACTTGATCCGTGCGGTGCAAGAAACCCATGAT
CGTGGTTTTGAGGCGCCGCTGCTTCTGGACGGTGACGGCCTGCTGGCGGAAGGCTCGGGCTTC
AATGTCGTCGTTATCAAGGATGGCGTTGTGCGCAGCCCGGGTCTGTGCCGCGCTGCCGGGCATCA
CGCGTAAAACCGTCTTGAAATTGCTGAGAGCCTGGGCCATGAAGCTATTTTGGCGGACATTACT
CTGGCGGAAGTGTGATGCGGATGAAGTTCTGGGTTGCACGACCCGCGGTGGCGTTTGGCCGT
TTGTTAGCGTCGACGGTAATCCGATCAGCGACGGTGTCCCGGGCCCGATCACGCAGTCAATTATC
CGTCGTTACTGGGAAGTGAACGTTGAGTCTAGCTCCTTGCTGACCCCGGTGCAGTACTAATAActcg
aggatccggctgctaacaagcccgaaggaagctgagttggctgctgccaccgctgagcaataactagcataacccttggggcctctaaa
cgggtctgaggggttttctgtaaggaggaactataccggatccacaggacgtctgcatgactagtctgctgtagcggcgcaat
aagcatcccaatggcgcgccgagcttggctcagcatggtcatagctgttctctgtgaaattgtatccgctcacaattccacacaacatacga
gccggaagcataaagtgtaaagcctgggggtcctaatagtgagtaactcacattaattgcgttgcgctcactgcccgttccagtcgggaaa
cctgtcgtgccagctgcattaatgaatcgccaacgcgcggggagagggcgttgcgtattgggctcttccgcttctcgtcactgactcgtg
cgctcggctcgtcggctcggcgagcggatcagctcactcaaaggcggtaatacggttatccacagaatcaggggataacgcaggaagaa
catgtgagcaaaaggccagcaaaaggccaggaaccgtaaaaaggccggttgcgtggttttccataggtccgccccctgacgagcatc
acaaaaatcgacgctcaagttagaggtggcgaaccgacaggactataaagataaccaggcgttccccctggaagctccctcgtgcgctct
cctgttccgaccctgcccttaccggatacctgtccgcttctccctcgggaagcgtggcgcttctcatagctcacgctgtaggtatcagttcgg
tgtaggtcgttgcctcaagctgggctgtgtgcacgaacccccgttcagcccagccgctgcgcttaccggtaactatcgtcttagtccaacc
ggaagacagacttatcgccactggcagcagccactgtaacaggattagcagagcaggtatgtaggcgggtctacagagttctgaagt
gtggcctaactacggctacactagaagaacagtatgttggatctgcgctctgctgaagccagttacctcggaaaaagagttgtagctctgatcc
ggcaaaaaaccaccgctggttagcgggtgtttttgttgaagcagcagattacgcgcagaaaaaaggatctcaagaagatcctttgatctt
tctacggggtctgacgctcagtggaacgaaaactcacgttaagggatttggctatgagattcaaaaaggatctcacctagatccttttaatta
aaaatgaagtttaaatcaatctaaagtatatatgagtaaaactggctgacagttagaaaaactcatcgagcatcaaatgaaactgcaattatc
atatcaggattatcaataccatattttgaaaaagccgttctgtaatgaaggagaaaaactcaccgaggtccataggatggcaagatcctgg
tatcggctcgcgattccgactcgtccaacatcaataaacctattaatccccctcgtcaaaaataaggttatcaagtgagaaatcaccatgagtga
cgactgaatccggtgagaatggcaaaagttatgcaattcttccagactgttcaacaggccagccattacgctcgtcatcaaaatcactcgcac
aaccaaacggtattcattcgtgattgcgctgagcagagacgaaatacgcgatcgtgttaaaaggacaattacaacaggaatcgaatgcaa
ccggcgaggaacactgccagcgcacatacaatattttcacctgaatcaggatattcttaataacctggaatgctgttttccagggatcgcagtg
gtgagtaaccatgcatcatcaggagtacggataaaatgctgtatggtcggaaagggcataaattccgctcagccagtttagctgacctctcatct
gtaacatcattggcaacgctaccttggcatgttcagaaacaactctggcgcatcgggcttccatacaatcgatagattgctgcacctgattgcc
cgacattatcgcgagcccattataccatataaatcagcatccatgttgaattaatcgcggcctagagcaagacgttcccggtgaaatggctc
atactcttctttcaatattatgaagcattatcaggggtattgtctcatgagcggatacatatttgaatgtattgaaaaataaacaataggggtt
ccgcgcacatttccccgaaaagtgccacctgacgtctaagaaaccattattatcatgacattaacctataaaaaataggcgtatcacgagggccctt
cgtc

Supplemental Data

Enzyme Assay and Activity:

In order to perform the enzyme activity assay in droplets, the reaction was first performed in bulk and analyzed in droplet format on the mass spectrometer. DNA was added to ivTT reaction mix at a 25:1 volume ratio and kept at room temperature on the benchtop. The reaction was quenched by freezing 20ul samples at regular time intervals. Droplet plugs were then formed from these samples in capillary using a syringe pump in withdraw mode as previously described.^[2] Because these plugs are formed and then immediately sprayed, they do not display the level of product ion transfer between droplets observed in bulk droplets (Figure 4A), and both the substrate and the product of the reaction may be monitored. The time course experiment shows that the ATA substrate concentration begins to decrease noticeably in the first few hours, and that it continues to drop over the course of a full day.

We elected to begin screening our droplet samples at the 3-4 hour mark because at this point, the reaction is roughly linear in its time-dependent response. At the start of this period, the library of active samples still overlaps with the inactive droplets. Over the course of a day of screening, the two populations begin to resolve more fully (Figure 4B). The observed signal spread is likely due in part to the variation between reaction start times inherent in the reagent addition setup. Using reagent addition, reactions are initiated over the course of 1-2 hours at approximately 10 additions per second. Altering the applied sorting ratio in the adaptive sorting threshold selects for different portions of the target population; a lower ratio selects for droplets showing higher substrate depletion, while a higher ratio is less selective.

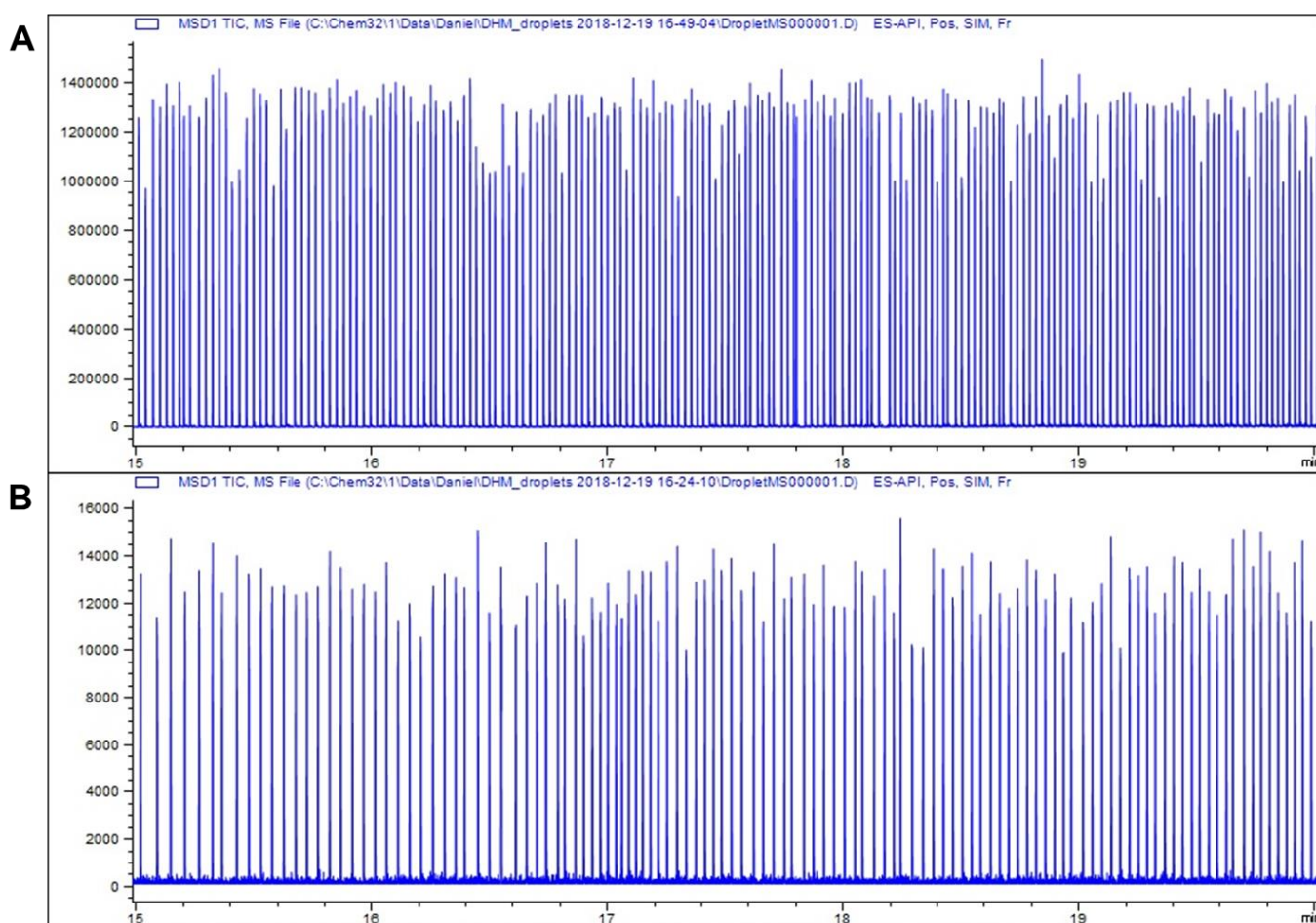


Figure S5: (A) ATA substrate amine is monitored in droplets stored in bulk and reinjected, and the raw ion trace shown. A distinct difference between active and inactive samples may be readily observed as a 20-30 percent decrease in signal intensity when monitoring the substrate of the reaction. (B) When monitoring the product ketone, the increase is not readily observable, likely due to transfer of the more hydrophobic ketone between droplets stored in bulk.

Droplet Leakage

Use of MS droplet analysis provides insight into the degree of molecular transfer between droplets. As such, while we have identified some small molecules (such as permanently charged neostigmine) which are remarkably stable in the droplets used here, most of the small molecules in this study exhibit some degree of transfer when stored in bulk. This is important in the case of the ATA Substrate, which was the target for our enzyme assay. While the substrate does transfer slower than the product of the reaction, the ATA substrate does indeed move between droplets. This can be readily observed by comparing the droplet signal distributions before and after mixing, as described in the section "Droplet MS Dynamic Range." Figure S6 shows this comparison in detail.

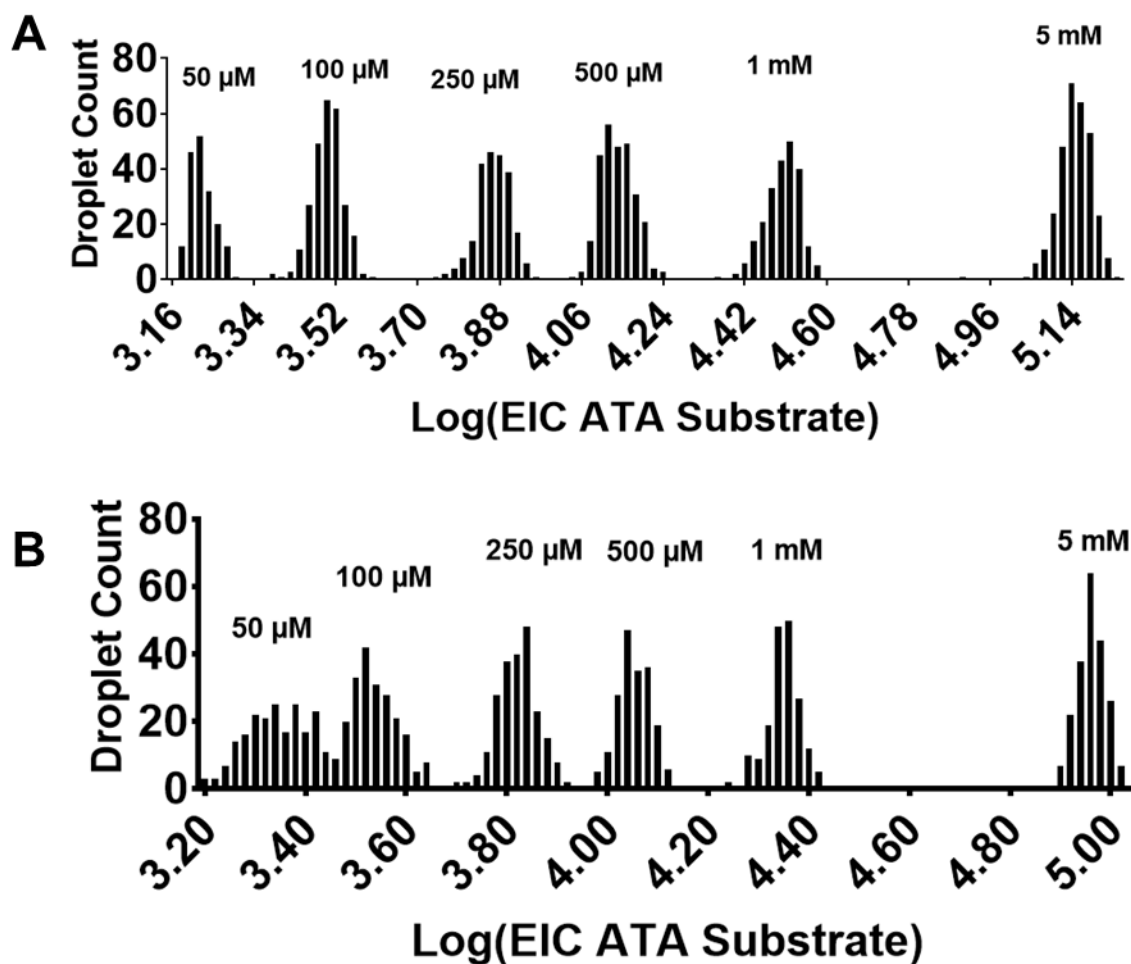


Figure S6: (A) binned signal intensity for the ATA substrate in ivTT droplets prior to mixing and (B) after mixing show that the hour of incubation between the datasets is sufficient for the distribution to shift slightly. The broadening of the droplet population histograms, and the rise in signal intensity for the lowest concentration samples suggest this is due to small amounts of substrate leaking from the higher concentration samples into the lower concentration samples, but may also stem in part from phenomena such as analyte degradation or droplet merging.

Extended Operation:

The MS was found to be capable of operation for upwards of 6 h of continuous screening at ~ 0.7 droplets per second. Signal variation or decline over the course of an extended run was observed predominantly for the ATA substrate amine (Figure S7), likely due to the steady loss of ATA substrate in the system as the active droplets consumed it and the inactive ones leaked it into their neighbors. This was addressed using adaptive thresholding to provide a real-time comparison to positive control data for sorting decision making.

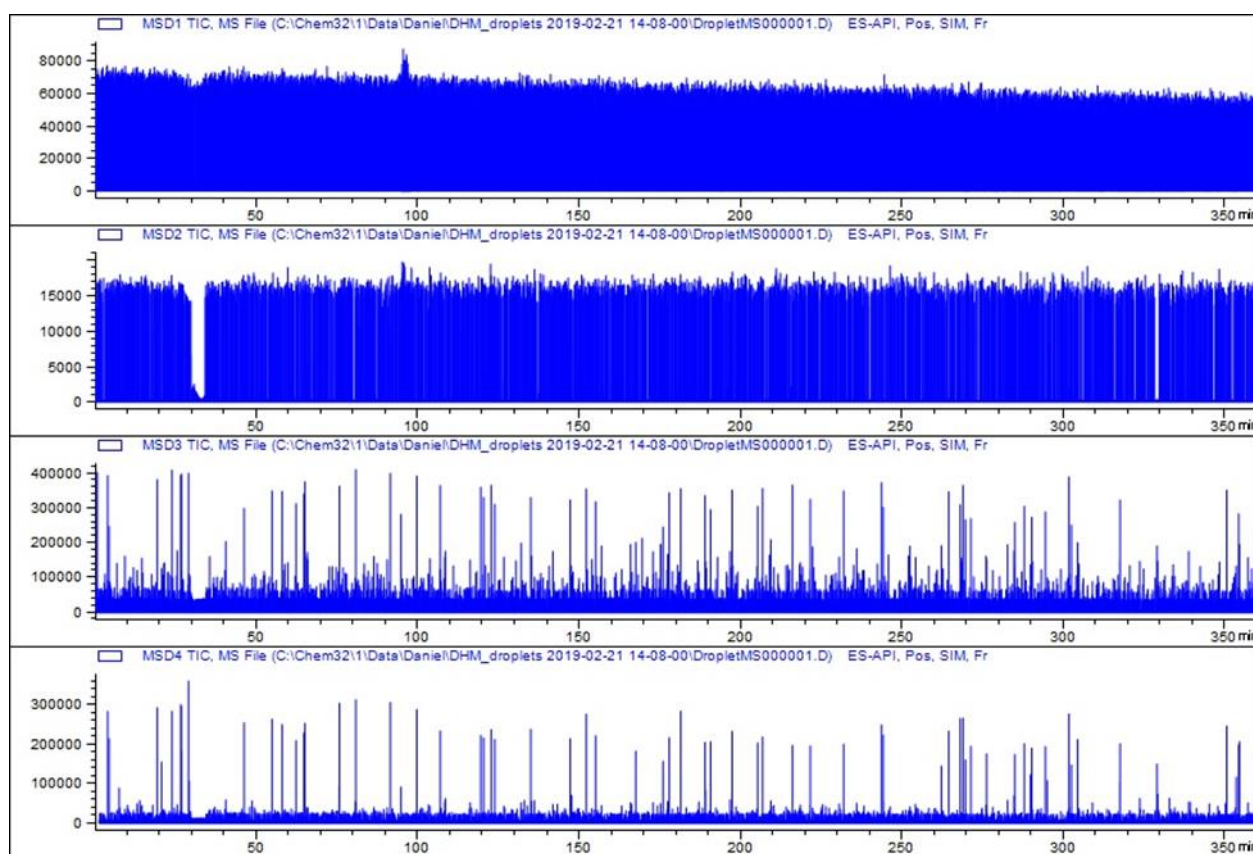


Figure S7: A 6 hour raw trace from a droplet sorting run monitoring 4 ions. The top trace tracks ATA substrate, the second trace tracks the marker droplet signal carnitine, the third trace tracks neostigmine from model library droplets, and the bottom trace tracks chlorocholine from positive control droplets. Nearly 15,000 peaks can be observed in this trace. A decrease in the ATA substrate signal of approximately 16% over the course of the run is accounted for during sorting using adaptive thresholding based off of the running average of ATA Substrate signal in droplets containing chlorocholine. A ~ 5 -min drop in signal at $t=30$ min is attributable to a large merged droplet passing through the system.

Sorting Ratio

The Sorting Ratio parameter is a tool that allows the user of the adaptive sorting algorithm to adjust the stringency of the MADS sorting. The advanced sorting algorithm uses the signals from a set of positive control droplets marked with an identifier ion to set an average expected value for active samples. When the sorting ratio is set to one, this average value is used as the threshold for selecting winner droplets. When the ratio is increased, the threshold rises, and higher signal reads meet the criteria for hits. For the purpose of our mock-evolution screen, we did not express an enzyme library, so the activity of our sample droplets was equal to the activity of the positive control droplets. This meant that a sorting ratio of 1 only collected approximately 50% of the sample droplets. In order to show isolation of high proportions of the sample population, we adjusted this sorting threshold to capture more of the targeted population of droplets, shown below.

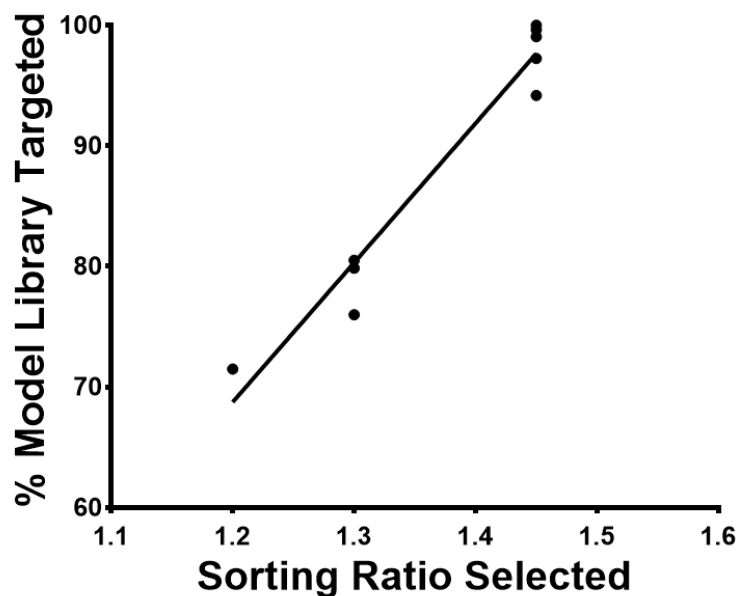
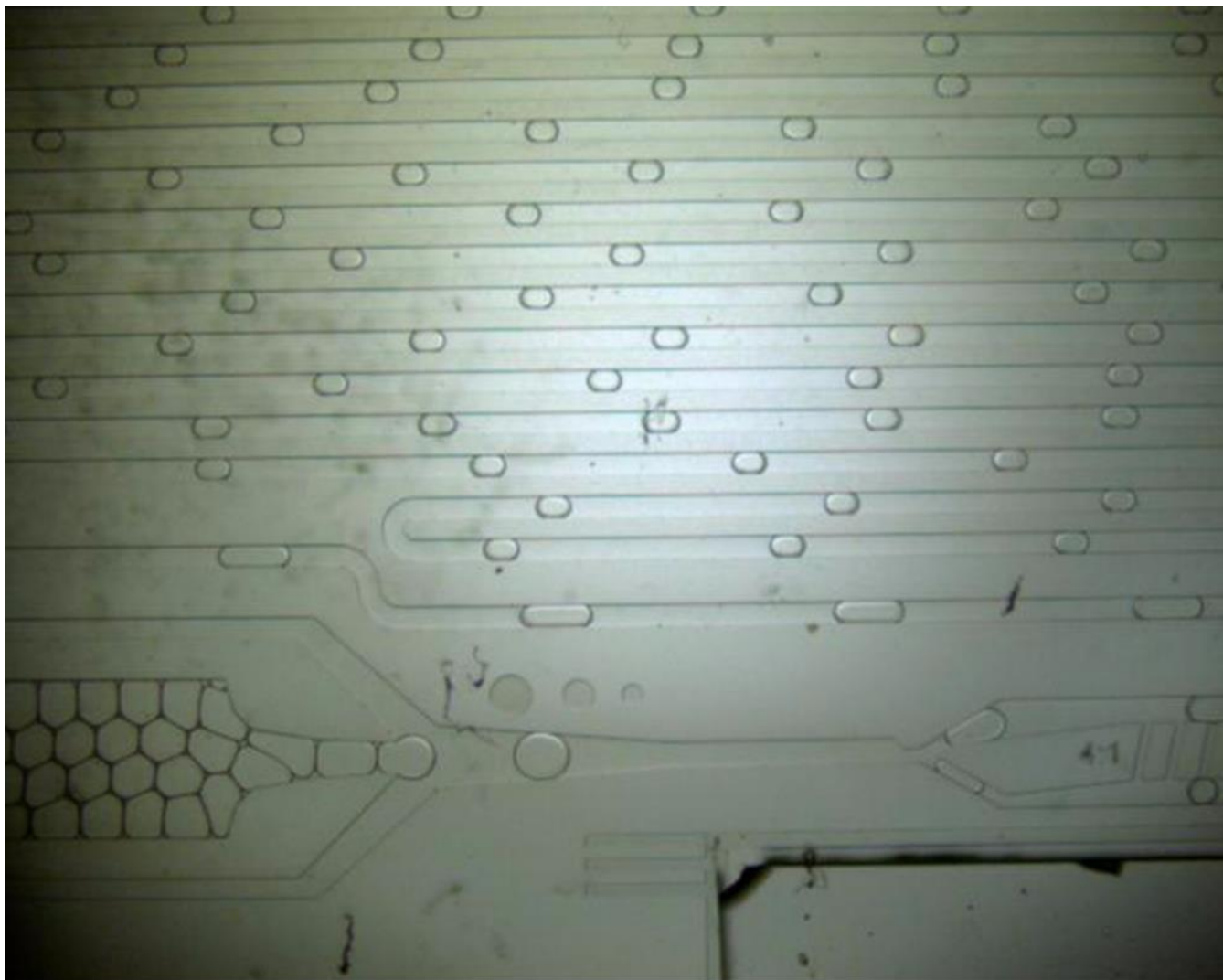
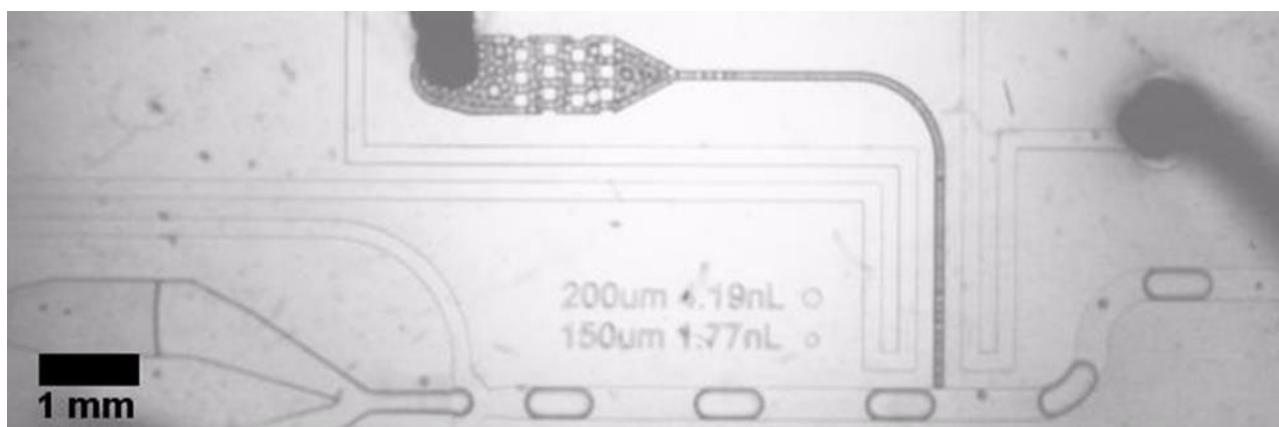


Figure S8: The fraction of model library droplets targeted for sorting as a function of selected sorting ratio. As the ratio is increased, more of the droplets in the model library pool meet the criteria for hits, and are selected for capture. In a true enzyme screen, this ratio would lie below 1 to capture only those samples performing better than the positive control.

Supplemental video descriptions:



Video S1. Droplets are pumped onto the MADS sorting device where they are asymmetrically split by a V-shaped bifurcation in the channel. The smaller daughter droplet remains on the device for downstream sorting while the larger is transported off of the device to the source of the MS and is ionized. Sorting of the droplets occurs outside of the image window of this video



Video S2: Small (~1 nL) DNA containing droplets are reinjected and paired with larger 25 nL droplets of ivTT generated on chip in a droplet merging device. The small droplets rapidly catch up to the larger ones in the channel. The paired droplets flow downstream to a pair of electrodes where a 1.5 kV AC electric field across two on-chip salt water electrodes disrupts the surfactant induced stability and causes the two to combine. The combined droplets are collected for reinjection and analysis.

References

- [1] H. Becker, C. Gartner, *Analytical and Bioanalytical Chemistry* **2008**, *390*, 89-111.
- [2] X. Diefenbach, I. Farasat, E. Guetschow, C. Welch, R. Kennedy, S. Sun, J. Moore, *Acs Omega* **2018**, *3*, 1498-1508.
- [3] A. Sciambi, A. Abate, *Lab on a Chip* **2014**, *14*, 2605-2609.

Author Contributions

D.H.M. designed and built the microfluidic devices, performed experiments as described, collected and analyzed the data. D.H.M. additionally wrote and edited the manuscript with input from collaborating researchers. M.W. wrote the code for the sorting microprocessor, built and modified the hardware for the sorting system, and wrote the descriptions for these systems included in the publication. B.F.M., helped devise the sorting alignment strategy and played a critical advisory role during early system setup. I.F. contributed with the design and optimization of the biology necessary for ATA 117 *in vitro* expression. E.G. played an advisory role in the early design and testing of the microfluidic devices. I.M., C.W., and P.D. served as advisors and administrators for the Merck-University of Michigan collaboration that allowed this work. S.S. and R.T.K. co-wrote the grant funding this work and contributed equally along with J.C.M as leading project administrators and scientific advisors.